



## POLITECNICO DI TORINO Repository ISTITUZIONALE

### A comparison of reduced-order techniques for complex interconnects modeling

#### *Original*

A comparison of reduced-order techniques for complex interconnects modeling / S. GRIVET-TALOCIA; I. MAIO; I. STIEVANO; F. CANAVERO. - STAMPA. - (2002), pp. 457-462. ((Intervento presentato al convegno IEEE International Symposium on Electromagnetic Compatibility tenutosi a Minneapolis, MN (USA) nel August 19-23, 2002.

#### *Availability:*

This version is available at: 11583/1409383 since: 2015-07-14T12:08:19Z

#### *Publisher:*

IEEE

#### *Published*

DOI:10.1109/ISEMC.2002.1032522

#### *Terms of use:*

openAccess

This article is made available under terms and conditions as specified in the corresponding bibliographic description in the repository

#### *Publisher copyright*

(Article begins on next page)

# A Comparison of Reduced-Order Techniques for Complex Interconnects Modeling

S. Grivet-Talocia, I. Maio, I. Stievano, F. Canavero

Dipartimento di Elettronica, Politecnico di Torino,  
Corso Duca degli Abruzzi 24, 10129, Torino, Italy  
{grivet,maio,stievano,canavero}@polito.it

## Abstract

*This paper compares the performance of different reduced-order modeling techniques applied to the description of complex interconnect structures. In particular, we analyze two main classes of modeling tools, the Block Complex Frequency Hopping (BCFH) and the Subspace-based State-Space System Identification (4SID) techniques. The strong and weak points of both methods are analyzed with particular attention to robustness and sensitivity to the control parameters of the algorithms.*

## INTRODUCTION

The high complexity of modern electronic systems calls for simplified modeling tools in order to perform system-level simulations for Signal Integrity and Electromagnetic Compatibility applications. Indeed, it is widely recognized that a system-level 3D electromagnetic simulation, including the effects of nonlinear drivers/receivers, is non-feasible even with today's powerful computing tools.

Order reduction techniques tackle the modeling problem under a different perspective. Various subparts (henceforth Devices Under Modeling, DUM) of the system are characterized separately at their accessible ports, either via numerical simulation or direct measurement. This procedure can be applied, e.g., to linear interconnects, junctions, packages, or connectors. Reduction techniques allow for the generation of simple equivalents mimicking the dominant input/output port behavior of the DUM. Such equivalents can be easily synthesized as SPICE subcircuits for system-level simulations, in order to include nonlinear effects of drivers/receivers. Next section gives a brief overview of the reduction techniques that are considered in this work. Numerical examples illustrating the strong and weak points of each method will follow.

## REDUCED-ORDER MODELING

In this paper we analyze the performance of two main classes of reduction techniques applied to complex interconnects structures characterized via transient time-domain port voltages and currents. These techniques are the well-known Block Complex Frequency Hopping (BCFH) algorithm and two different variations of the so-called Subspace-

based State-Space System Identification (4SID).

## Block Complex Frequency Hopping (BCFH)

The BCFH algorithm [1, 2] is a moment matching order reduction method leading to estimate the true set of poles of the DUM within a prescribed bandwidth of interest. This is achieved by computing the moments of port transfer functions at several complex expansion points  $\{\alpha_k\}$ . The theory of Padé approximants is then used to determine the poles set, which in turn is used to represent each transfer function with a partial fraction expansion, whose residues are computed by a least squares fit. The obtained models have a solid physical foundation, because their poles are approximations of the actual natural frequencies of the DUM. The synthesis of a lumped equivalent circuit is a standard problem once the poles-residues approximation is known. In the following we assume as known the BCFH algorithm, pointing the reader to references [1, 2] for further details.

The main weak point of such approach for present application lies in the high sensitivity of the poles estimation algorithm to the duration of the observation time. The recording time for port variables should indeed allow for all transients to be extinguished, since the moments  $\mu_{\alpha_k}^n$  of some port waveform  $x(t)$  can be only computed through numerical discretization of the integral

$$\mu_{\alpha_k}^n = \int_0^\infty \frac{(-t)^n}{n!} x(t) e^{-\alpha_k t} dt, \quad (1)$$

where, however,  $x(t)$  is only known up to a maximum time  $T$ . This applies when  $x(t)$  is obtained via numerical simulation or through direct measurement. Only an estimate of the moments is therefore available through

$$\hat{\mu}_{\alpha_k}^n = \int_0^T \frac{(-t)^n}{n!} x(t) e^{-\alpha_k t} dt. \quad (2)$$

The effects of this truncation error worsen with an increasing order  $n$  of the moment. Conversely, such effects can be partially compensated by tuning the real part of the expansion centers  $\alpha_k$  in order to force the magnitude of the integrand to be negligible beyond  $T$ . Namely, there is a minimum (positive) allowed value of  $\mathcal{R}(\alpha_k)$ . The following procedure can be used to estimate it.

First, let us suppose that the waveform  $x(t)$  is the response of a linear system characterized by some poles and residues. Therefore, the asymptotic behavior of its magnitude is dominated by the real part  $\sigma_0$  of its dominant pole, i.e.,

$$|x(t)| \simeq e^{\sigma_0 t}. \quad (3)$$

A rough estimate of  $\sigma_0$  is easily obtained, e.g., by performing a least squares logarithmic fit of the cumulative energy of  $x(t)$ . Assuming this asymptotic behavior, we can substitute Eq. (3) in the expression of the  $n$ -th order moment and compute analytically the relative error  $\delta_{\alpha_k}^n(T)$  due to truncation. The expression of this error requires the use of the incomplete Gamma function. However, a truncated asymptotic expansion leads to the following estimate

$$\delta_{\alpha_k}^n(T) \simeq e^{-(\alpha_k - \sigma_0)T} \sum_{r=0}^n \frac{(\alpha_k - \sigma_0)^r}{r!} \quad (4)$$

This expression can be used to determine the location of the expansion centers  $\alpha_k$  in the complex frequency plane allowing a negligible truncation error for given order, truncation time, and dominant pole of the response.

As a final remark, we note that the larger the real part of the expansion centers, the least significant will be the truncation error. Unfortunately, this condition worsen the behavior of the Padé convergence, leading to a possibly failed poles estimation. This can be mathematically justified noting that the system poles (obviously constrained to have negative real part) are "seen" from a far location. Therefore, poor convergence is expected. Consequently, a careful compromise must be adopted to balance the truncation error and the pole-convergence properties. This strategy will be used throughout this paper in conjunction with the BCFH algorithm.

### Subspace-based State-Space System Identification (4SID)

The 4SID methods [8] determine a state-space representation of the DUM via direct identification of the state matrices. The identification algorithm makes use of highly reliable numerical tools (QR and SVD decompositions), and proves less sensitive to time-domain truncation of the port signals with respect to BCFH (see the numerical examples). Some details on the identification algorithm follow.

The DUM is represented in Fig. 1. Some linear interconnect structure is considered at a limited number  $m$  of accessible ports. The structure is of distributed nature, therefore an infinite number of poles would be required for an accurate representation of the input/output relation  $Y(s) = H(s)U(s)$ , where  $U$  and  $Y$  are vectors collecting all port variables. The goal is to identify a reduced-order linear lumped system, characterized by  $n$  poles and represented by the state matrices  $\{A, B, C, D\}$ , such that all input/output transfer functions  $\hat{H}(j\omega)$  approximate the true ones over a specified bandwidth  $|\omega| < \Omega$ . The starting point is a set of transient

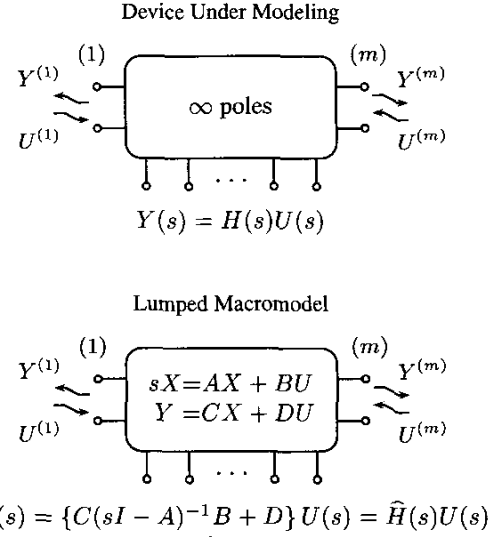


**Figure 1: State-space based macromodeling. Arrays  $Y$  and  $U$  collect input and output variables at all ports.**

waveforms of outputs  $y_k$ , where  $k$  denotes the time index with a suitable sampling time  $T_s$ , subject to some combination of input waveforms  $u_k$ .

Since the input/output sequences are sampled, it is convenient to focus our attention on the discrete-time system,

$$\begin{cases} x_{k+1} &= \tilde{A}x_k + \tilde{B}u_k \\ y_k &= \tilde{C}x_k + \tilde{D}u_k \end{cases} \quad (5)$$

where  $x$  denotes the set of internal discrete-time states. This formulation allows us to use the several theoretical results available for system identification of discrete-time systems [6]. In order to simplify the presentation of the main algorithm, we first consider a Single-Input Single/Output (SISO) system. Generalization to a large number of ports will follow.

First, we note that the above system may be rewritten in matrix form as

$$\mathcal{Y} = \Gamma \mathcal{X} + \Phi \mathcal{U}, \quad (6)$$

where  $\mathcal{U}, \mathcal{Y}, \mathcal{X}$  denote block Hankel matrices of input, output, and state time sequences, respectively. We recall that given some sequence  $z_k$ , the corresponding Hankel matrix is defined as  $(Z)_{ij} = z_{i+j-1}$ . In the above expression  $\Gamma$  represents the observability matrix

$$\Gamma = \begin{bmatrix} \tilde{C} \\ \tilde{C}\tilde{A} \\ \tilde{C}\tilde{A}^2 \\ \vdots \end{bmatrix}, \quad (7)$$

while  $\Phi$  is a Toeplitz matrix of impulse responses. A remarkable feature of Eq. (6) is that the output matrix is expressed as

a linear combination of state matrix and input matrix. Therefore, a suitable projection of  $\mathcal{Y}$  onto some linear space orthogonal to  $\mathcal{U}$  leads to an estimate of the observability matrix, which in turn can be used to estimate the state matrix  $\hat{A}$ . Some details follow, whereas a more complete formulation can be found in [8].

One of the most convenient ways to perform this projection is through the following  $RQ$  factorization

$$\begin{bmatrix} \mathcal{U} \\ \mathcal{Y} \end{bmatrix} = \begin{bmatrix} R_{11} & 0 \\ R_{21} & R_{22} \end{bmatrix} \begin{bmatrix} Q_1 \\ Q_2 \end{bmatrix} = RQ, \quad (8)$$

where  $Q^T Q = I$ . If we post-multiply the various terms in Eq. (6) by  $Q_2^T$ , we get

$$\mathcal{Y}Q_2^T = R_{22} = \Gamma \mathcal{X}Q_2^T, \quad (9)$$

where we used the orthogonality relations  $Q_2 Q_2^T = I$  and  $Q_1 Q_2^T = 0$ . A consistent estimate for the observability matrix  $\Gamma$  may be obtained by performing the SVD decomposition

$$R_{22} = \hat{\Gamma} \Sigma V^T. \quad (10)$$

The number of relevant singular values in  $\Sigma$  gives an estimate of the effective rank of the observability matrix, and consequently the order  $n$  of the state-space system to be identified. The corresponding columns of  $\hat{\Gamma}$  form the reduced-order observability matrix. Using now Eq. (7), both matrices  $\tilde{C}$  and  $\tilde{A}$  are easily found.

Several approaches [4, 7, 8] can now be used to estimate the remaining matrices  $\tilde{B}$  and  $\tilde{D}$ , like, e.g., a time-domain or frequency-domain least squares fit. Once all four state space matrices are known a straightforward discrete-to-continuous time conversion leads to the model representation of Fig. 1. We remark that for multiport circuit elements, all input and output sequences at the ports can be collectively used in a block matrix form in order to obtain the model realization in one step. All ports must be persistently and contemporarily excited for this task. However, due to the size of the involved matrices, this procedure can only be applied to cases with a limited number of ports (e.g., up to some ten ports). For a large number of ports a modified procedure is to be preferred. This procedure is described next.

### Column-oriented 4SID Method

Reduced-order macromodeling of linear multiport elements with a large number of ports can be tackled using a slightly modified version of the above-described 4SID technique. We repeat all steps of the algorithm up to the computation of the matrix  $\tilde{A}$ . Then, we determine its eigenvalues  $\lambda_i$  and consequently the poles of the continuous-time macromodel through

$$p_i = \frac{1}{T_s} \ln(\lambda_i). \quad (11)$$

Each transfer function of the reduced-order macromodel will have poles taken from the above set.

In case of a DUM with many ports, the best numerical accuracy was obtained by repeating  $m$  times the poles estimation with excitation at a single port at the time, henceforth the denomination *column-oriented 4SID* that we adopt for the algorithm. All output sequences resulting at the DUM ports from a single excitation are used collectively in a block-matrix form. The obtained  $m$  sets of estimated poles, one set per excited port, are then post-processed by a suitable clustering algorithm to extract the global poles set for the entire multiport macromodel. It should be noted that when real-world packages are considered, often each set of independently estimated poles can actually be used directly for the entire macromodel, thereby skipping the clustering step. This will be illustrated by the examples in the forthcoming section.

Once the poles of the DUM macromodel are known, the partial fraction expansion

$$\hat{H}(s) = \sum_i H_i \frac{1}{s - p_i} + H_\infty \quad (12)$$

is considered, where  $H_i$  are unknown matrices of residues and  $H_\infty$  is a matrix collecting the direct coupling constants between all DUM ports. These matrices are easily obtained by a linear least squares fit from original input/output data sequences. This fit can be performed either on time-domain sequences or using frequency-domain data. Some examples will be provided in the numerical results section.

The final step in the algorithm is the identification of the state matrices  $\{A, B, C, D\}$  from poles and residues. Once such matrices are found, they can be used to synthesize SPICE-like equivalent circuits through well known techniques. The particular form of the state matrices depends on some arbitrary choice, since several realizations are possible. In this work we compute the Gilbert's representation from the residue matrices as proposed in [3]. This solution guarantees a final macromodel characterized by minimum complexity.

The following remarks are important. First, there is no theoretical limit in the number of DUM ports. The algorithm has been developed in such a way that the critical operations related to the poles estimation are performed without using all ports information at once, thus leading to very accurate poles estimates. It is well known that this feature is the key factor for an accurate least-squares approximation and for the subsequent steps of the macromodeling algorithm. Second, since the above algorithm is very accurate, the enforcement of the passivity for the DUM macromodel can be performed a posteriori by applying small corrections if some passivity test fails [5].

### NUMERICAL RESULTS

In this Section, the BCFH and the 4SID techniques are applied to the characterization of two test structures and a realistic 32-port package. In all the tests carried out, the DUMs are stimulated by gaussian pulses and their transient

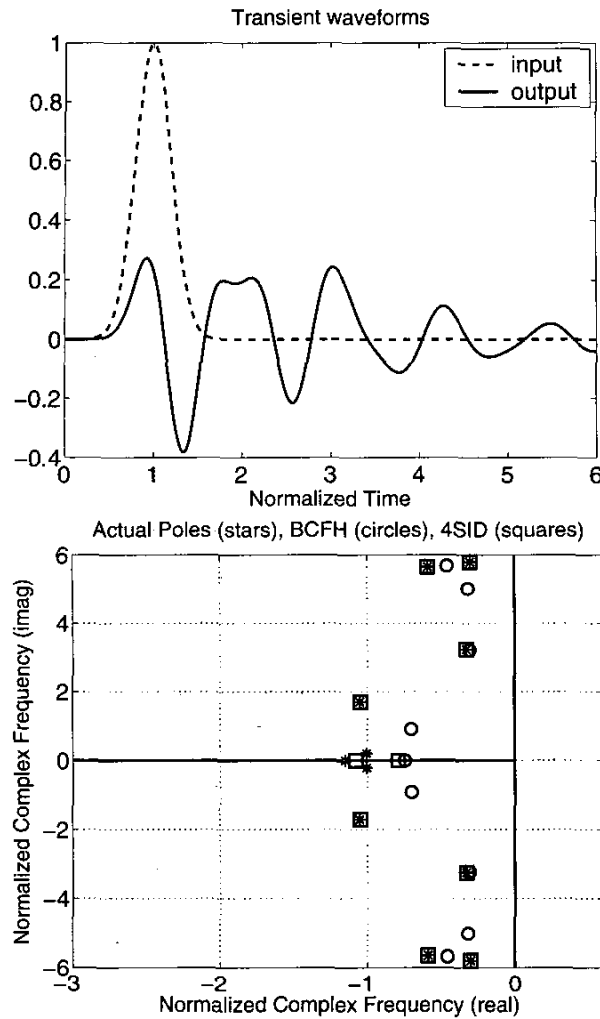


**Figure 2: Test linear system with truncated input and output transient waveforms.**

responses are recorded and used in the estimation processes. In the first example we consider a synthetic DUM defined by a transfer function with known poles and residues. The top panel of Fig. 2 shows the gaussian input and the output transient waveforms used by the BCFH and the 4SID estimation process. In this case we consider the basic 4SID technique where the  $B$  and  $D$  matrices are obtained via least squares fit in the frequency domain. The bottom panel reports the poles estimated by both algorithms compared to the original ones. As expected, the evident truncation of the time window leads to a rough estimate of the poles through BCFH, even after optimization of the expansion points. On the contrary, 4SID is more robust and less sensitive to the duration of time sequences. Poles estimation is the most important part of both methods, since a representative set of poles generally leads to good approximations of the DUM responses.

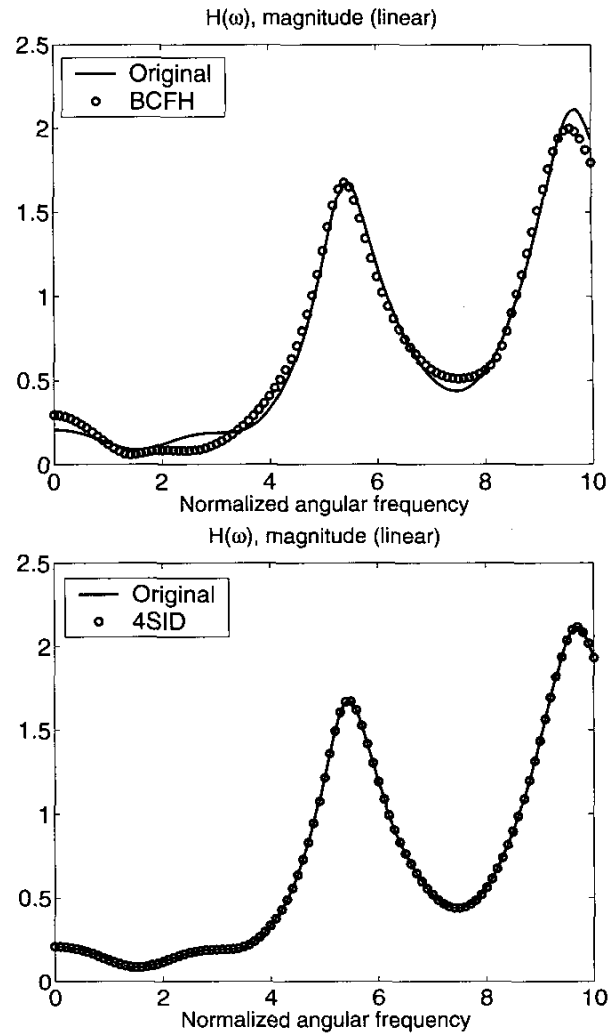


**Figure 3: Performance of BCFH and 4SID algorithms applied to a test case (Figure 2) with truncated input and output transient waveforms.**

This can be clearly appreciated in Fig. 3, where the transfer function predicted by the two methods is compared to the reference one.

As a second example we consider the three-port structure of Fig. 4 consisting of lumped and distributed elements. In this case the time window is set long enough to avoid truncation of the transient responses and again, the two approaches are considered and applied. The estimation of matrices  $B$  and  $D$  in 4SID are computed via least squares fit in both the time-domain and the frequency-domain, in order to point out the differences. Left panel of Fig. 5 shows the comparison between the actual poles of the DUM and the poles estimated for the set  $S_{12}$  through BCFH. It should be noted that BCFH is an inherently scalar approach and that any scattering pa-

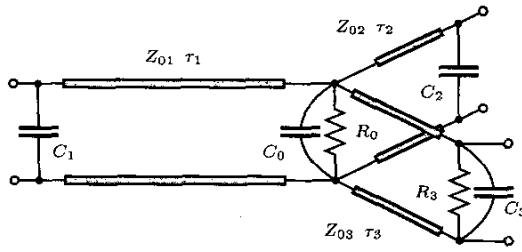


Figure 4: Three-port test structure composed of lumped and distributed elements.

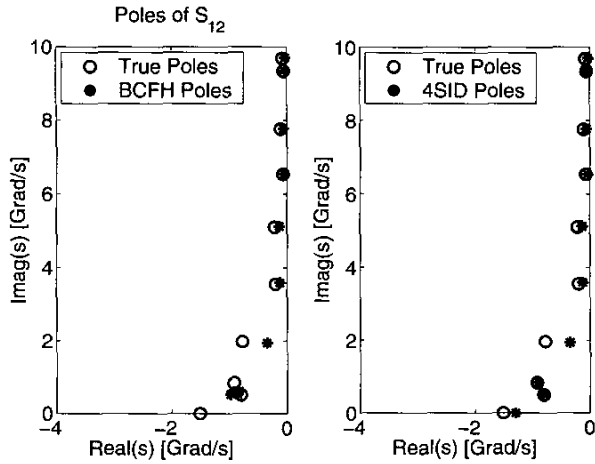


Figure 5: Poles detected by BCFH and 4SID for the structure depicted in Figure 4.

parameter requires its own set of poles. Right panel of Fig. 5 shows a similar comparison for the global poles estimated by 4SID. This example confirms that a sufficient duration of the time sequences leads to a good poles estimation also for BCFH. Consequently, the performance of both methods is comparable in terms of accuracy. This is illustrated in Fig. 6, which compares the original and the predicted  $S_{12}$  scattering parameter. Conversely, a noticeable difference between the two methods is in the computing time needed by the reduction process. In this case 4SID results much faster than BCFH, due to the long duration of the port waveforms.

Finally, in the last example we consider a realistic 32-port package structure. Only the results of the column-oriented 4SID algorithm are presented, since this is the only method that we find reasonably applicable to multiport elements with many ports. Indeed, the poles are more accurate when identified through 4SID, in a shorter computing time. Figure 7 shows the transient scattering waves at the DUM ports obtained through a full wave FDTD simulation. These waveforms are used to estimate the global set of poles (one real and four complex poles), and to perform least squares fit for

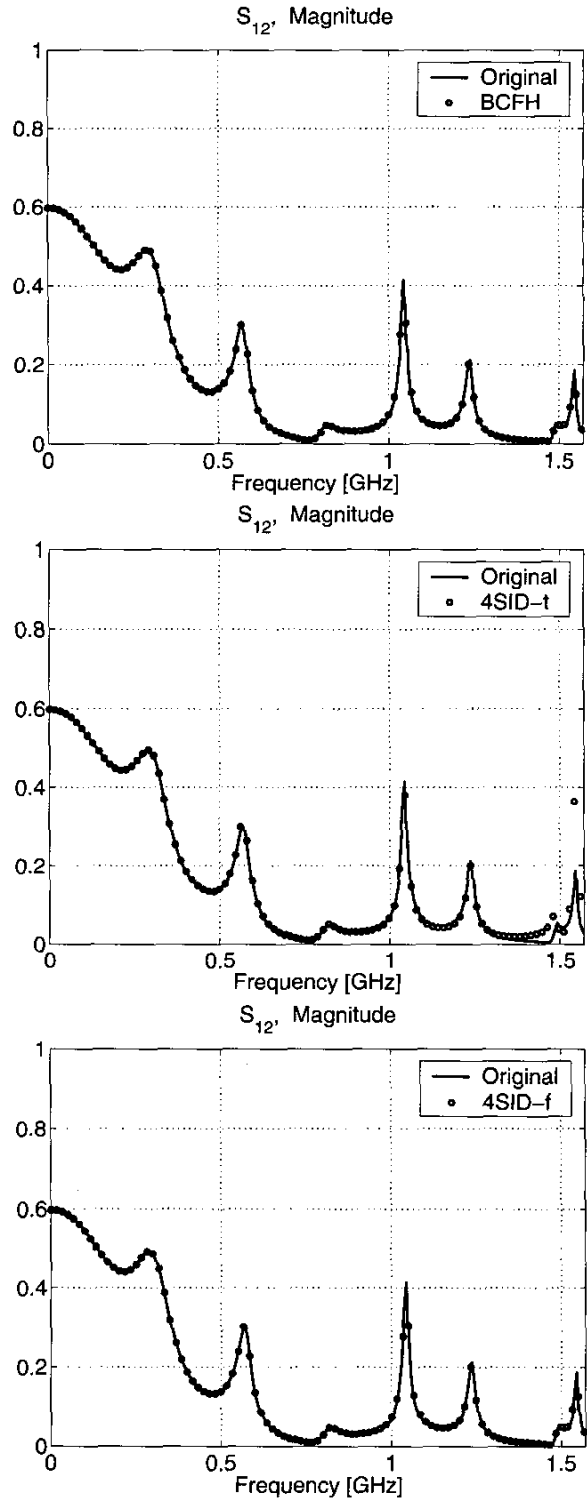


Figure 6: Scattering element  $S_{12}$  obtained by BCFH (top panel), 4SID with time-domain fit (middle panel), and 4SID with frequency-domain fit (bottom panel).

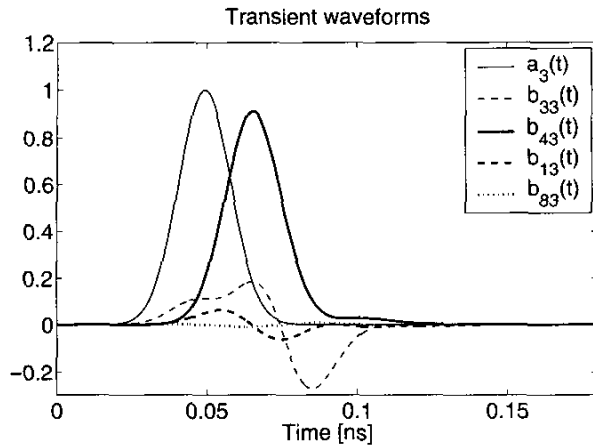


Figure 7: Transient scattering waveforms obtained by a full-wave FDTD simulation of a 32-port package structure.

computation of the residues. Figure 8 shows the comparison between some predicted scattering parameters and the corresponding reference ones. We see that a very good accuracy is obtained.

## CONCLUSION

We conclude noting that, based on the above examples, the proposed column-oriented 4SID method gives probably the best compromise between accuracy, complexity, and applicability to a wide range of structures, including packages and interconnects with a very large number of ports. The algorithm seems quite robust to numerical errors and to truncation of the transient waveforms used by the macromodeling steps. Therefore, it is expected that in the near future optimized versions of the algorithm will allow macromodeling of more and more complex structures.

## REFERENCES

- [1] R. Achar, M. Nakhla, and E. Chiprout, "Block CFH – a model-reduction technique for multiport distributed interconnect networks," *Proc. of ECCTD'97*, pp. 396–401, Sept. 1997.
- [2] R. Achar, P. K. Gunupudi, M. Nakhla, and E. Chiprout, "Passive interconnect reduction algorithm for distributed/measured networks," *IEEE Trans. Circ. and Sys.—II: analog and digital sig. proc.*, vol. 47, pp. 287–301, Apr. 2000.

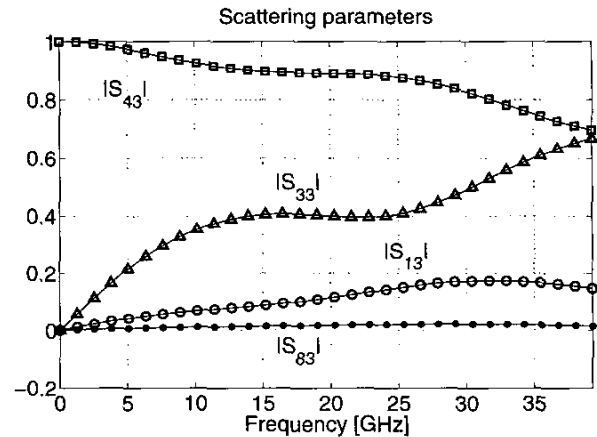


Figure 8: Scattering elements for the 32-port package structure (solid lines: reference; symbols: macromodel).

- [3] R. Achar, M. Nakhla, "Minimum realization of reduced-order high-speed interconnect macromodels", in *Signal Propagation on Interconnects*, H. Grabinski and P. Nordholz Eds., Kluwer, 1998.
- [4] C. T. Chou, M. Verhaegen, "Subspace Algorithms for the Identification of Multivariable Dynamic Errors-in-Variables Models," *Automatica*, Vol. 33, No. 10, pp. 1857–1869, 1997.
- [5] B. Gustavsen, A. Semlyen, "Enforcing passivity for admittance matrices approximated by rational functions", *IEEE Trans. Power Systems*, vol. 16, 2001, 97–104.
- [6] L. Ljung, *System identification: theory for the user*, Prentice-Hall, 1987.
- [7] V. Verdult, M. Verhaegen, C. T. Chou, M. Lovera, "Efficient Subspace-Based Identification of MIMO Bilinear State Space Models," *Proceedings of the International Workshop on Advanced Black-Box Techniques for Nonlinear Modeling: Theory and Applications*, Leuven, B, July 8–10, 1998.
- [8] M. Viberg, "Subspace-based methods for the identification of linear time-invariant systems," *Automatica*, Vol. 31, No. 12, pp. 1835–1851, 1995.